Selective Formation of Bi-Component Arrays Through H-Bonding of Multivalent Molecular Modules

By *Luc Piot, Carlos-Andres Palma, Anna Llanes-Pallas, Maurizio Prato, Zsolt Szekrényes, Katalin Kamarás, Davide Bonifazi,** and *Paolo Samorì**

Here, the formation of discrete supramolecular mono- and bi-component architectures from novel and multivalent molecular modules bearing complementary recognition moieties that are prone to undergo multiple H-bonds, such as 2,6-di(acetylamino)pyridine and uracil residues, is described. These nanostructured H-bonded arrays, including dimeric and pentameric species, are thoroughly characterized in solution by NMR, in the solid state by FT-IR, and at the solid–liquid interface by means of scanning tunneling microscopy. The employed strategy is extremely versatile as it relies on the tuning of the valency, size, and geometry of the molecular modules; thus, it may be of interest for the bottom-up fabrication of nanostructured functional materials with sub-nanometer precision.

1. Introduction

Nanostructured materials with tailor-made properties and functions can be developed by exploiting the supramolecular approach through molecular recognition.[1–4] In fact, the hierarchical self-assembly of multivalent molecular modules through the concerted action of multiple non-covalent interactions represents a very powerful approach as it makes possible the simultaneous organization of various molecular systems into intrinsically defect-free 2D architectures featuring a long-range order.[5–11] The structural and functional properties of the final supramolecular assemblies result from the assembling information stored in the molecular components, which are dictated by the interplay of both geometrical and conformational constraints, and by the presence of complementary recognition end-groups. To this end it is therefore vital to use shape-persistent molecular modules dictating well-defined geometries to the supramolecular ensemble. Hitherto a large variety of interactions have been employed in order to hold together molecular modules forming targeted self-assembled mono-component architectures at surfaces including dipolar forces,[12–17] coordination bonds,[18–24] H-bonds,[25–39] and more recently covalent interactions.[40–44] Among the proposed approaches, the use of H-bonding[45] is very promising since this type of interaction features very high directionality and selectivity, along with a reversible character, providing access to a vast variety of sophisticated functional assemblies and materials barely accessible through conventional covalent synthesis. To this end, the self-association between pre-programmed moieties attached to the peripheral sites of the molecular modules has been extensively employed.[5–11,46] Alongside mono-component assemblies, complementary recognizing moieties forming hybrid H-bonds have been also used to strengthen the hetero-molecular junctions assembling asymmetric molecular units. By adopting this strategy, it is possible to form numerous 2D multi-component monolayers as porous networks,[11,46] such as those composed by perylene tetracarboxylic di-imide (PTCDI),[47] cyanuric acid[48] or bis-functionalized uracyl[49] mixed with melamine, bi-component wires and ribbons from conjugated molecular modules,[50] intermixed monolayers containing trimesic acid (TMA) and 1-undecanol,[51] or DNA bases,[52] and finally discrete complexes based on isophthalic acids[41] or perylene dyes.[53]

Here we report on the use of specific complementary H-bonding units selected for their ability to form three parallel (i.e., triple), yet reversible, H-bonds. To accomplish this goal we have chosen conformationally-rigid π-conjugated molecules exposing 2,6-di(acetylamino)pyridine or uracil recognition end-groups.[54–56] We provide unambiguous evidence that the accurate design of the multivalent molecular building blocks allows the versatile generation of complex and discrete assemblies, such as dimers and pentamers, featuring a controlled geometry. These

[*] Dr. D. Bonifazi, A. Llanes-Pallas, Prof. M. Prato
Dipartimento di Scienze Farmaceutiche
Università degli Studi di Trieste
Piazzale Europa 1, 34127 Trieste (Italy)
E-mail: davide.bonifazi@fundp.ac.be
and
INSTM UdR di Trieste, Università degli Studi di Trieste
Piazzale Europa 1, 34127 Trieste (Italy)
Dr. D. Bonifazi
Department of Chemistry, University of Namur
Rue de Bruxelles 61, 5000 Namur (Belgium)
Prof. P. Samorì, Dr. L. Piot, C. A. Palma
ISIS-CNRS 7006, Université Louis Pasteur
8 allée Gaspard Monge, 67000 Strasbourg (France)
E-mail: samori@isis-ulp.org
Z. Szekrényes, Dr. K. Kamarás
Research Institute for Solid State Physics
P.O. Box 49, 1525 Budapest (Hungary)
and
Optics Hungarian Academy of Sciences
P.O. Box 49, 1525 Budapest (Hungary)

DOI: 10.1002/adfm.200801419

assemblies have been thoroughly characterized in solution by ^{1}H NMR, in the solid state by FT-IR, and at the solid–liquid interface by in situ scanning tunneling microscopy (STM) studies.

2. Synthesis and Assembling Behavior in Solution

The design of organic-based functional patterns relies on the development of new methodologies to predictably assemble programmed molecular modules via directional non-covalent interactions.[57] As shown in Figure 1, our strategy involved the synthesis of multivalent molecular modules (molecules **1**–**3**) that expose at their peripheries complementary recognition sites incorporating H-bonding donor and acceptor moieties. In particular, aiming at mimicking the complementary base pairing of the DNA structure, we have engineered molecular modules featuring 2,6-di(acetylamino)pyridine moieties for the selective and reversible recognition of uracil-bearing derivatives.[55,60,61] Specifically, the hetero-molecular recognition between these units is mediated via triple H-bonds established between the NH–N–NH (DAD) functions of the 2,6-di(acetylamino)pyridines and the CO–NH–CO (ADA) imidic groups of the uracil derivatives. Notably, the amide groups in 2,6-di(acetylamino)pyridyl functions prefer to adopt a *trans* conformation, with the carbonyl *anti* oriented to the pyridine nitrogen, preventing the formation of dimeric $(\mathbf{1})_2$ species due to strong repulsive secondary electrostatic interactions. The uracil residues conversely, can self-associate forming weakly-bonded homo-molecular species ($K_a < 10\ M^{-1}$) such as $(\mathbf{2})_2$ (see dimer geometry in Fig. 1a).[62]

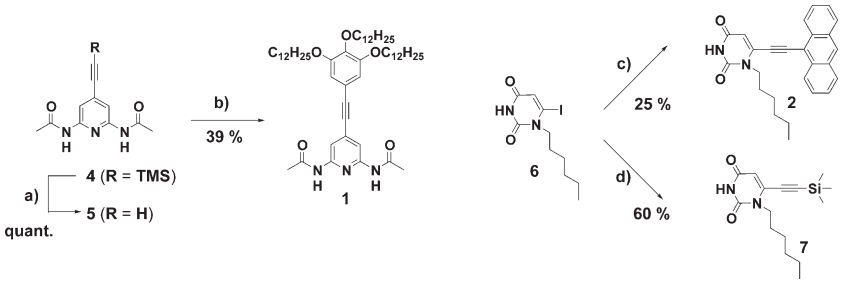

Scheme 1. Synthesis of H-bonding recognition modules. Reagents and conditions: a) KOH, MeOH, RT, 40 min; b) 1-bromo-3,4,5-tri(dodecyloxy)benzene, $[Pd(OAc)_2]$, CuI, PPh_3, i-Pr_2NH, THF, 85 °C, 12 h; c) 9-ethynyl-anthracene, $[Pd(OAc)_2]$, CuI, PPh_3, i-Pr_2NH, THF, 12 h; d) $[Pd(PPh_3)_2Cl_2]$, CuI, Et_3N, toluene, TMSA. Ac_2O = acetic anhydride; TMSA = trimethylsilyl acetylene; i-Pr_2NH = diisopropylamine.

We have thus decided to functionalize the recognition units with alkyl chains in order to facilitate their investigation both in solution and at the solid–liquid interface and also with aromatic units to provide optical properties to the systems. The different modules (**1**–**3**) bearing complementary H-bonding moieties used in our study are outlined in Figure 1. Molecules **2** and **3** feature one and four terminal uracil moieties, respectively, which are connected to a central aromatic ring through a rigid ethynyl spacer. Molecule **1**, which is terminated with a 3,4,5-tri(dodecyloxy) benzene group, bears one 2,6-di(acetylamino)pyridyl moiety and thus acts as a complementary unit toward the complexation of modules **2** and **3**.

Tetratopic 1,3,6,8-tetrakis[(1-hexylurac-6-yl)ethynyl]pyrene **3**, 1-hexyl-6-iodouracil **6** and ethynyl derivatives, **4** and **5**, were synthesized following the protocol recently developed by us.[58,59] All assembling molecular modules have been synthesized by Sonogashira-type cross-coupling reactions[63] starting from the respective ethynyl derivatives (Scheme 1). Pd-catalyzed cross-coupling reaction between 1-bromo-3,4,5-tri-(dodecyloxy)benzene[64] and ethynyl-pyridine **5** in the presence of copper iodide and $[Pd(PPh_3)_4]$ afforded molecular module **1**. The presence of long aliphatic chains endows the assembling modules with high solubility and enhanced affinity for highly ordered pyrolytic graphite (HOPG) surfaces.[65,66] Direct Sonogashira-type coupling of iodo-uracil **6** with 9-ethynylanthracene (synthesized following a slightly modified procedure than that reported by Dang and Garcia Garibay)[67] and TMSA gave uracil-anthracene and ethynyl-uracil derivatives **2** and **7**, respectively. All compound structures were assessed by ESI mass-spectrometry, ^{1}H- and ^{13}C-NMR, UV-VIS, and IR spectroscopy.

Since the aromatic groups attached to the recognition moieties could strongly influence their self-assembly behavior (i.e., the K_a), we investigated the association properties of complementary silylated precursors **4** and **7** ([**4**·**7**]) and of silylated precursor **4** with 1-hexyl-6-[(anthracen-9-yl)ethynyl]uracil **2** ([**4**·**2**]). Finally, the complexation between the complementary

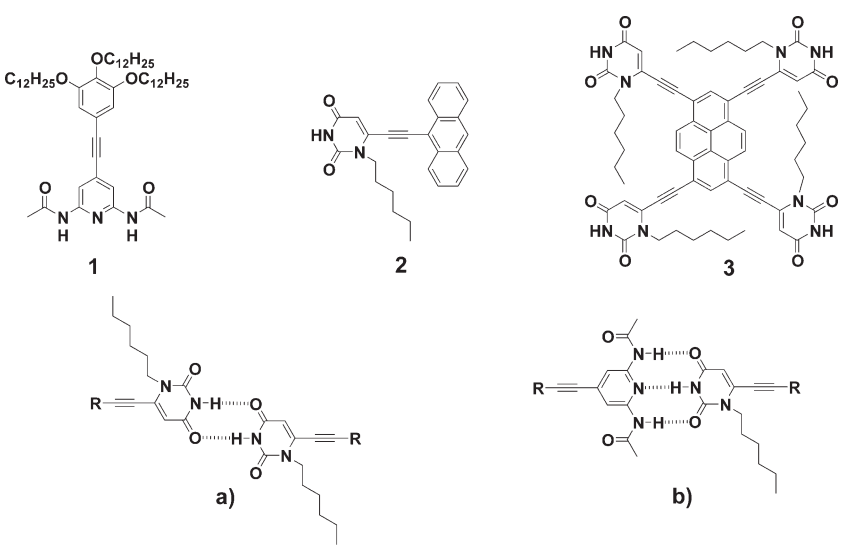

Figure 1. Chemical structures of the molecular modules bearing complementary H-bonding recognition sites investigated in this work. Molecule **3** was synthesized according to recently developed synthetic protocols [58, 59]. a) One of the three possible homo-association geometries between two uracil end-groups and b) hetero-association geometry between di(acetylamino)-pyridine and uracil residues.

Table 1. Calculated stoichiometries and association constants (K_a) for the H-bonded dimers in $CDCl_3$ at 295 K. The reported values are the average of at least two consecutive experiments.

Complex	Stoichiometry	K_a [M^{-1}]	$-\Delta G°$ [kJ mol^{-1}]
4 + **7** ⇔ **[4·7]**	1:1	8.94×10^2	16.6
4 + **2** ⇔ **[4·2]**	1:1	2.01×10^3	18.7
1 + **2** ⇔ **[1·2]**	1:1	1.21×10^3	17.4

pair **1** and **2** ([**1·2**]) was also studied. The complexes were characterized in $CDCl_3$ by means of ^{1}H-NMR-based titrations and Job plots to determine the association strength and the assembly stoichiometry, respectively (Table 1; also see the titration curves and Job plots in the Supporting Information). For the three binary supramolecular systems, the Job plots showed a 1:1 binding stoichiometry. For the titration studies the concentration of the host (uracil derivatives) was kept constant (5 mM) and the change of the chemical shift of the imide N–H protons has been recorded as a function of the increase of the guest concentration (i.e., the 2,6-di(acetylamino)pyridine derivatives). As expected, a significant downfield shift of the imidic protons due to the complexation of the uracil was observed. The association constants were extrapolated from the binding isotherms as created from the NMRTit HG software for the Apple Mac OS X operating system.[68] The associations constant values (Table 1), 8.94×10^2 for [**4·7**], 2.01×10^3 for [**4·2**], and 1.21×10^3 for [**1·2**], revealed to be in the same order as those reported in literature for similar systems,[55,60,69] suggesting that the functionalization of the uracil and of the 2,6-di(acetylamino)pyridyl groups did not alter the H-bonding recognition properties.

3. IR Measurements

Vibrational spectroscopy is an established method to detect and measure H-bond strengths.[70,71] H-bonds can be sensitively detected in the infrared absorption region, either by directly measuring the vibrations of the H-bonds in the far IR,[72] or by their effect in the N–H and C=O stretching regions of the spectra.[73] The unambiguous assignment of the hetero-molecular H-bond-related features is not straightforward, due to the complexity of the systems under study, in particular given that molecule **2** forms a dimer through homo-molecular association in the solid-state and in solution. Such homo-molecular dimers exhibit similar vibrations to those of the hetero-molecular complexes. However, the vibrational modes can be determined exactly: i) upon comparison of the differences in the spectra of the starting materials and those of the H-bonded adducts and ii) from variable temperature spectra, because at high temperatures (120–150 °C) the H-bonds become weaker or entirely disrupted.[74]

Although the 2,6-di(acetylamino)pyridine-uracil pair has been extensively used for the formation of supramolecular polymers,[54–56] only a limited number of reports deal with spectroscopic investigations in the IR region for such hetero-molecular dimers.[62] The supramolecular dimer [**1·2**] was prepared by mixing an equimolar solution of molecules **1** and **2** followed by solvent evaporation. The spectra were recorded by mixing the as-obtained powder with KBr. Figure 2 reveals that the [**1·2**] dimer spectrum is not the spectral sum of its constituents **1**+**2**, but essential differences appear in the typical H-bond perturbed regions. Figure 2b displays the N–H and C–H stretch region in detail. The peaks at 2 800–2 900 cm^{-1}, corresponding to C–H stretching vibrations,[73] remain unaffected upon the formation of the H-bonding interactions. The full spectra of all materials are shown in the Supporting Information. In contrast, the peaks between 3 000 and 3 500 cm^{-1} are strongly perturbed. The spectral sum of **1** and **2** features homo-molecular H-bonds typical of $(\mathbf{2})_2$, as evidenced from the peaks at 3 039 and 3 082 cm^{-1}.

The peak at 3 465 cm^{-1} can be assigned to the stretching frequency of the H-bond free N–H groups existing in 2,6-di(acetylamino)pyridine moiety (**1**). This frequency is comparable to that found in the vapor phase spectra of 2-aminopyridine[75] and matrix isolation spectra of thymine.[76] In dimer [**1·2**], this feature disappears completely. The features located at 3 039 and 3 082 cm^{-1} are also missing in the spectra of the supramolecular dimer, ruling out any significant homo-molecular H-bonding in the powders. In contrast, new features appear at typical N–H stretch modes,[77] i.e., those at 3 070, 3 224, and 3 283 cm^{-1}. These modes are redshifted when compared to the H-bond free N–H frequency of the 2,6-(diacetylamino)pyridine moiety at 3 465 cm^{-1}, providing evidences for the formation of H-bonds.[78] Thus the as-formed hetero-molecular dimer [**1·2**] appears as having all three nitrogen atoms bridged through H-bonds (Fig. 1b).

The region between 1 200 and 1 700 cm^{-1}, typical of skeletal vibrations, C=O stretching and N–H in-plane bending modes can be analyzed along the same lines (Fig. 2a). We have indicated in the figure the unique modes of the constituents and of the complex. The temperature-dependent spectra of dimer [**1·2**] detailed in Figure 3 prove that the peaks at 1 210, 1 329, 1 464, 1 501, 1 581, and 1 690 cm^{-1} are considerably affected by the H-bonds. Among these, three peaks (positioned at 1 214, 1 464, and 1 501 cm^{-1}) coincide with the features assigned by Rozenberg et al. to the uracilic vibrations with major contributions from N–H in-plane bending modes,[79] and one (located at 1 690 cm^{-1}) with the uracilic C=O stretching as reported by Barnes et al.[73] This further confirms the formation of three

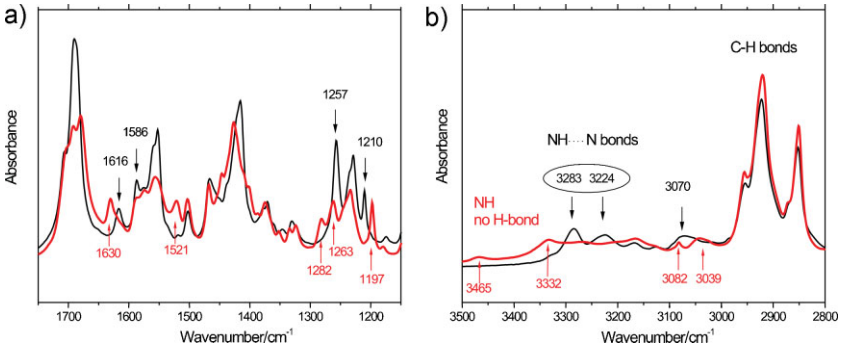

Figure 2. a) Mid-frequency-range IR spectra of dimer [**1·2**] (black) and of the sum **1**+**2** (red) of the separated molecular constituents. b) IR spectra in the N–H and C–H stretching region of dimer [**1·2**] (black) and the sum **1**+**2** (red) of its separated molecular constituents. All spectra were recorded on powders ground in KBr pellets at RT.

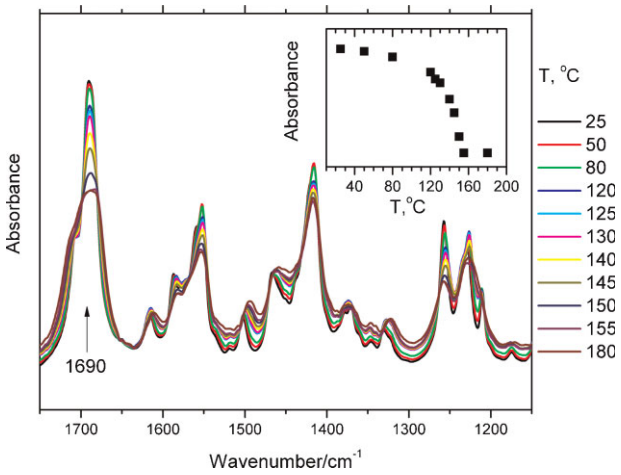

Figure 3. Mid-frequency spectrum and its dependence on the temperature for dimer [**1**·**2**] in KBr pellets. Inset: peak intensity of the 1 690 cm^{-1} mode as a function of the temperature.

parallel H-bonds between molecules **1** and **2**. As discussed by Iogansen,[78] the intensities of the vibrational bands are correlated to the strength of the H-bonds. The inset of Figure 3 shows the intensity of the 1 690 cm^{-1} peak as a function of temperature; as expected, profound changes in the typical temperature range (between 120 and 150 °C) of H-bond weakening occur.[74]

Figure 4 summarizes the H-bond related structures in the IR spectrum upon comparison of [**1**·**2**] dimer at room temperature (rt) and 180 °C and the spectral sum of its constituents. Additionally, the far-IR spectral region, where the direct vibrations of the H-bonds appear, are also displayed. Far-IR spectra have been taken on neat powders between polyethylene disks. The vibrational mode at 119 cm^{-1} originates from the 2,6-(diacetylamino)pyridine moieties of molecule **1** (see Supporting Information) thus corresponding to the N–H···N bond.[80] A new feature also appears in the spectra of complex [**1**·**2**] at 217 cm^{-1}, which, based on analogy with other systems,[72] we have tentatively assigned to the N–H···O bond.

4. STM Measurements at the Solid–Liquid Interface

STM measurements were then performed in order to provide a proof, in real space, of the formation of H-bonded complexes on atomically flat surfaces. Molecular modules **1** and **2** were designed to undergo physisorption on HOPG into highly ordered monolayers at the solid–liquid interface. Physisorption on graphite was promoted by the presence of alkyl-chain side groups in both molecular structures. Moreover, molecule **2** also incorporated an anthracenyl moiety that is known to exhibit a good affinity for graphite. This enhanced affinity of both molecules for the HOPG could be expected to lead to a lowering of the molecules mobility on the surface, facilitating the sub-molecularly resolved characterization of the patterned surface by STM. Furthermore, the alkyl chains grafted on both molecules **1** and **2** promoted a good solubility in different, highly apolar,

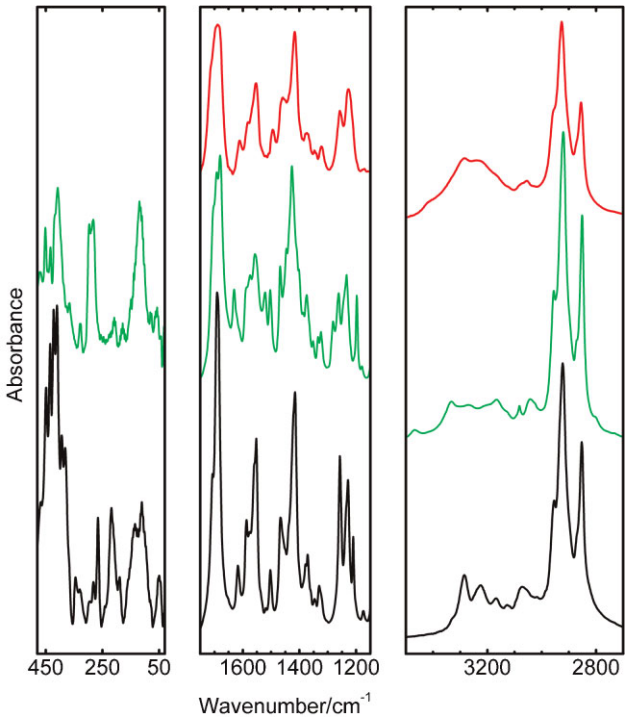

Figure 4. Comparison of the IR spectrum of complex [**1**·**2**] at 25 °C (black) and at 180 °C (red) with that of the sum **1**+**2** (green) of its constituents alone at rt. In the far IR (left panel), the vibrations of the hetero-molecular H-bonds appear at 120 and 217 cm^{-1}. In the C=O stretching region (middle panel), both homo-molecular $(\mathbf{2})_2$ and hetero-molecular [**1**·**2**] intermolecular interactions influence the spectra between 1 200–1 300 and 1 500–1 750 cm^{-1} regions. Similarly, the signatures of N–H···N bonding interaction appear between 3 200 and 3 400 cm^{-1}.

organic solvents (i.e., 1-phenyloctane or *n*-tetradecane), which are typically employed for STM measurements at the solid–liquid interface. Finally, both molecules have two chemical structures which can be expected to give rather different STM contrasts when physisorbed on HOPG. Thus, in the case of co-adsorption, this should facilitate the differentiation of one type of molecules from the others, since the long alkyl-chains provide in many cases a lower tunnelling contrast than the aromatic moieties.[81]

Both molecules were first characterized as mono-component monolayers. A solution of molecule **2** dissolved in *n*-tetradecane was deposited on the surface. The STM images in Figure 5a display the formation of a highly ordered crystalline monolayer; in view of the resonant tunneling between the Fermi level of the substrate and the frontier orbitals of the ad-molecule, the brighter features can be ascribed to the anthracene moieties, whereas the darker parts of the image can be attributed to the alkyl chains.[81] The corresponding packing motif shown in the cartoon reveals the occurrence of homo-association, that is, the formation of two (i.e., double) N–H···O bonds among adjacent molecules thus forming $(\mathbf{2})_2$ dimers. Similarly, molecule **1** was deposited from a 1-phenyloctane solution on the HOPG surface, resulting in the formation of a monolayer with a lamellar structure displayed in Figure 5c. Three different types of tunnelling contrasts can be observed in the STM image: i) dark gray parallel lines, which can be ascribed to the alkoxy side-chains, ii) brighter rod-like features,

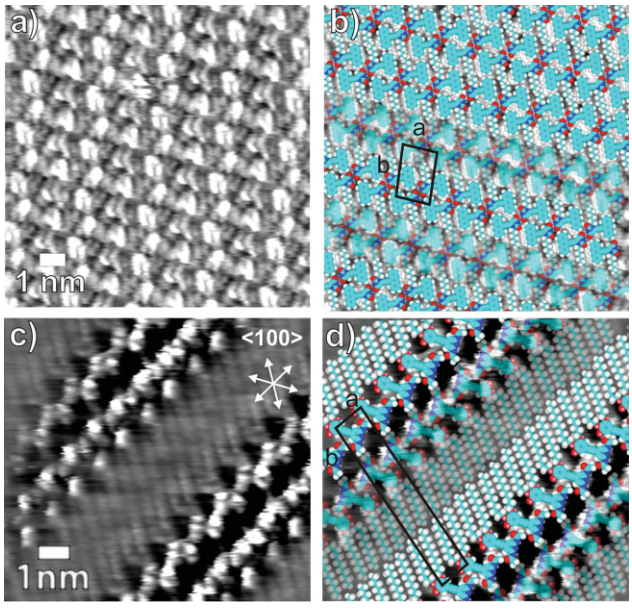

Figure 5. STM images recorded at the graphite-solution interface. a) Height image of mono-component monolayers of molecule **2** and b) its proposed packing model. Unit cell parameters: $a = 1.4 \pm 0.1$ nm, $b = 2.2 \pm 0.1$ nm, $\alpha = 83° \pm 2°$, leading to an area $A = 3.1 \pm 0.3$ nm^2. c) Current image of monolayer of **1**, and d) its proposed packing motif showing that one alkoxy chain per molecule is not adsorbed on the surface. Unit cell parameters: $a = 1.0 \pm 0.1$ nm, $b = 5.9 \pm 0.1$ nm, $\alpha = 80° \pm 2°$, $A = 5.8 \pm 0.7$ nm^2. Tunneling parameters: for (a) average tunneling current (I_t) = 5 pA; bias voltage (U_t) = 750 mV, and for (c) $I_t = 10$ pA; $U_t = 1000$ mV.

that can be attributed to the conjugated moieties, and iii) a darkest contrast region between two rows of molecules. The arrows superimposed in Figure 5c indicate the underlying ⟨100⟩ HOPG orientation, which in turn matches the alignment of the aliphatic chains. In this case, the self-assembly is mostly governed by commensurability of the aliphatic chains with the HOPG substrate.[65,66] The high resolution achieved in the STM image clearly shows the characteristic linear signature of the individual alkyl chains, providing unambiguous evidences that one alkyl chain per molecule is not adsorbed on the surface but is rather back-folded in the supernatant solution, similarly to other alkyl-substituted organic systems physisorbed at the HOPG-solution interface[82] (for more detail see Fig. S3, Supporting Information). The STM image also reveals that the molecules belonging to one lamella facially expose the 2,6-di(acetylamino)pyridine moiety separated by a gap featuring a dark contrast. Such a gap may either be uncoated or covered with solvent molecules featuring a high dynamics on a timescale faster than the STM scanning, since its size suggests the absence H-bonds between molecules belonging to neighboring lamellae. At the intra-lamellar level, a weak O···HC hydrogen-bonding between adjacent 2,6-di(acetylamino)pyridine moieties may further stabilize the packing motifs.

Given the previously described associating propensity of molecules **1** and **2** in solution, as proved by NMR and FT-IR measurements, we extended our investigation to the co-adsorption of the modules at the solid–liquid interface. Solutions of molecules **1** and **2** were prepared in a mixture of 1-phenyloctane and toluene in order to increase the solubility of both components and to thus obtain homogeneous phases. The drop-casting of a 1:1 molar solution of **1** and **2** led to the adsorption of only molecule **2** on the basal plane of the graphite. This was evidenced by STM measurements showing the presence of a packing motif identical to that observed for the mono-component monolayers of molecule **2** in Figure 5a. This may be due to the stabilization of the monolayer of molecule **2** through homo-association forming supramolecular $(\mathbf{2})_2$ dimers. Under these experimental conditions molecule **1** remains in the 3D supernatant solution. Making use of a solution with a 1:10 molar ratio where molecule **1** is in excess (i.e., 0.4 mM of **2** and 4 mM of **1**), the equilibrium can be shifted to favor the formation of hetero-molecular supramolecular assemblies on the surface (Fig. 6a). The STM image reveals bright rods, the length of which is in good accordance with the cumulative contour lengths of molecule **2** and the conjugated fragment of molecule **1**, whereas the darker areas correspond to the adsorbed alkoxy chains of molecule **1**. In Figure 6b a molecular pattern of the molecules **1** (in blue) and **2** (in yellow) is proposed. In combination with the underlying STM image, it provides strong evidences for the existence of [**1**·**2**] dimers on the surface. We notice that in the inter-lamellar region the central alkoxy chain of molecule **1** has the freedom to adopt different conformations: the STM images do not provide unambiguous information about their packing, thus they may even be back-folded in the supernatant solution. Given that such a dimerization through H-bonding interactions has been also detected in solution by NMR measurements, it is most likely that the dimers are formed in solution and then transferred to the graphite surface as bi-component entities.

To prove the general applicability of this approach for the co-deposition of two or more components at the solid–liquid interface, we extended our study to a multitopic molecular module, pre-programmed to generate more complex geometries. In this view, the multitopic molecule **3** has been synthesized[59] in order to use a tetrasubstituted pyrene module as a cornerstone for the self-assembly. According to its geometry, one can expect that the recognition and the combination of each uracil unit at the four extremities of molecule **3** with one 2,6-di(acetylamino)pyridine of molecule **1** results in the generation of pentameric species [$(\mathbf{1})_4$·**3**]

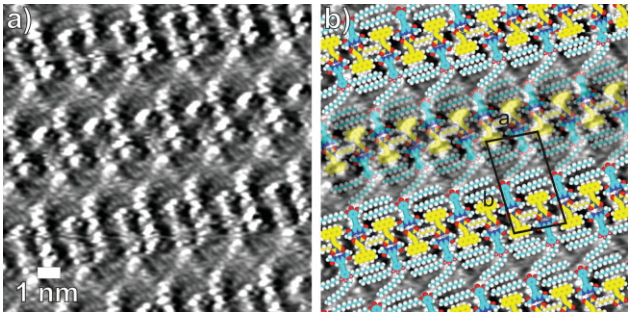

Figure 6. a) STM current image of the monolayers formed by mixing molecule **1** and **2** on the HOPG-solution interface. Each dimer is composed by one molecule **1** (blue) and one molecule **2** (yellow). a) The unit cell is depicted in black. b) Proposed model of the assembly. Unit cell parameters: $a = 2.3 \pm 0.1$ nm, $b = 4.2 \pm 0.1$ nm, $\alpha = 84° \pm 2°$, leading to an area $A = 9.6 \pm 0.8$ nm^2. Tunneling parameters: $I_t = 55$ pA; $U_t = 400$ mV.

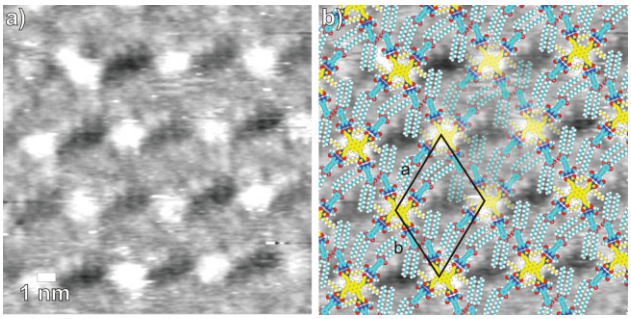

Figure 7. a) STM height image of the monolayer formed with molecules **1** and **3**. The addition of a solution of molecule **3** on top of an already existing monolayer of **1** is followed by the formation of complexes. b) Proposed model showing that each complex is composed by one molecule **3** surrounded by four molecules **1**. Unit cell parameters: $a = 4.8 \pm 0.1$ nm, $b = 4.2 \pm 0.1$ nm, $\alpha = 64^\circ \pm 2^\circ$ leading to an area $A = 18.1 \pm 2.4$ nm^2. Tunneling parameters for (a): $I_t = 10$ pA; $U_t = 500$ mV.

displaying a ''Saint Andrew'' cross-like shape. Upon physisorption of only molecule **3** on HOPG, large ordered domains were observed (Fig. S4, Supporting Information). The molecules were found to interact with their four neighbors through two double (i.e., double) H-bonding interactions. The resulting unit-cell is rhombic and contains one molecule (see Fig. S5, Supporting Information). Surprisingly, by using the previous procedure for the formation of dimers, it was not possible to obtain any hybrid complexes based on molecule **1** and **3** on the surface. In fact it was found that only molecule **1** adsorbed on the surface, even at different molar ratios (ranging from 1:1 up to 1:10 of molecule **1**:**3**). We therefore opted to employ a different procedure based on two steps deposition. First a monolayer of molecule **1** was formed upon deposition of a drop of a 0.5 mM solution in 1-phenyloctane to HOPG, and the resulting structure was thoroughly characterized by STM. Then, an additional drop of a solution containing molecule **3** in 1-phenyloctane (conc. 0.2 mM) was deposited on the surface. After an overnight annealing at rt, the wet film was studied in situ by STM. Figure 7a exhibits a STM image of the resulting monolayer where three main contrasts are present, the brighter one being mainly attributed to the aromatic cores of both molecule **3** and **1**, whereas the medium and lower contrast regions correspond to the alkyl chains and to possible vacancies of the monolayer or to unpacked solvent molecules featuring high dynamics on a timescale faster than the STM scanning.

The proposed molecular model is displayed in Figure 7b: it consists of discrete self-assembled complexes, each of them comprising one molecule **3** surrounded by four molecules **1** through the formation of three triple H-bonds, thereby forming pentameric supramolecular structures [(**1**)$_4$·**3**]. The measured unit-cell area is 18.1 nm^2, which is bigger than the calculated Van der Waals area of 13.9 nm^2 occupied by one pentameric complex indicating that some parts of the surface either remain uncoated or covered with highly dynamic solvent molecules.

5. Conclusions

In summary, we have reported the synthesis of multivalent molecular modules based on 2,6-di(acetylamino)pyridine and uracil derivatives that have been pre-programmed to undergo hetero-association through the formation of H-bonds among the moieties exposed at the periphery of their chemical structure. FT-IR characterization as well as ^{1}H NMR showed the formation of supramolecular dimers of molecules **1** and **2** that are held together by three triple H-bonds. A careful and rational design of the molecules allowed the generation of pre-programmed highly ordered 2D self-assembled monolayers, the latter being studied at the solid–liquid interface by STM. High-resolution images made it possible to unravel the packing of bi-component H-bonded complexes on the surface. The presented results provided large evidences for the high flexibility of the approach, which can be used for the selective binding of molecular guest into different polygonal bi-component architectures. This finding represents a proof of principle of the approach and opens perspectives towards the formation of nanoporous and multi-component supramolecular networks that can be exploited to confine and address functional molecules at determined locations.

6. Experimental

Synthesis: NMR spectra were obtained on a Varian Gemini 200 spectrometer (200 MHz ^{1}H NMR and 50 MHz ^{13}C NMR) and on a Jeol JNM-EX400 (400 MHz, ^{1}H NMR). Chemical shifts are reported in ppm using the solvent residual signal as an internal reference ($CDCl_3$: $\delta_H = 7.26$ ppm, $\delta_C = 77.16$ ppm. The resonance multiplicity is described as s (singlet), d (doublet), t (triplet), m (multiplet), br (broad signal). IR spectra (KBr) were recorded on a Perkin Elmer 2000 spectometer by Mr. Paolo de Baseggio. Electron impact (EI) mass spectrometry measurements were performed on a Ion trap GCQ Finnigan Thermoquest at 70 eV by Dr. Fabio Hollan. Melting points (m.p.) were measured on a Büchi SMP-20. Chemicals were purchased from Aldrich, Fluka, and Riedel and used as received. Solvents were purchased from JTBaker and Aldrich, and deuterated solvents from Cambridge Isotope Laboratories. General solvents such as Toluene, THF, and NEt_3 were distilled from Na, Na/benzophenone, and CaH_2 respectively. Compounds **2** [58] and **3**–**6** [59] were synthesized following the protocols reported by us previously. 1-bromo-3,4,5-tri(dodecyloxy)benzene, [64] and 9-ethynylanthracene [67] were prepared according to literature procedures.

*2,6-Di(acetylamino)-4-{[3,4,5-tri(dodecyloxy) phenyl]ethynyl}pyridine (**1**)*: Dry THF (15 mL) and i-Pr_2NH (15 mL) were added to a Schlenk tube. The solution was degassed by one ''freeze-pump-thaw'' cycle. 1-Bromo-3,4,5-tri(dodecyloxy)benzene (0.5 g, 0.71 mmol), $[Pd(OAc)_2]$ (0.081 g, 0.36 mmol), CuI (0.093 g, 0.49 mmol), and PPh_3 (0.149 g, 0.57 mmol) were then added and the solution degassed a second time. Finally, 4-ethynylpyridine-2,6-di(acetylamino)pyridine **4** (0.190 g, 0.92 mmol) was added, the reaction mixture degassed one more time and the whole mixture stirred overnight at 85 °C under Ar. The resulting brown mixture was filtered over celite and washed with CH_2Cl_2 (30 mL). Removal of the solvents under vacuum and purification of the crude by CC (cyclohexane/EtOAc 7:3 first and then 5:5) yielded compound **1** (0.29 g, 39%) as a pale orange solid. m.p. 78–80 °C; ^{1}H NMR (400 MHz, $CDCl_3$, δ): 8.0 (s, 2H; Ar-*H*), 7.7 (br, 2H; CH_3CONH-Ar), 6.7 (*s*, 2H; Ar-*H*), 3.9 (t, 6H; $OCH_2(CH_2)_{10}CH_3$), 2.2 (*s*, 6H; CH_3CONH-Ar), 1.8 (m, 6H; $OCH_2CH_2(CH_2)_9CH_3$), 1.3 (br, 54H; $OCH_2CH_2(CH_2)_9CH_3$), 0.8 (*t*, 9H; $O(CH_2)_{11}CH_3$); ^{13}C NMR (50 MHz, $CDCl_3$, δ): 168.71, 152.88, 149.19, 138.56, 136.8, 116.27, 111.09, 110.28, 94.71, 86.16, 73.522, 69.08, 31.91, 30.28, 29.69, 29.63, 29.57, 29.38, 29.34, 29.29, 26.06, 24.68, 22.67, 14.10; IR (cm^{-1}): $\nu = 3466.7$, 3332.0, 2955.7, 2919.2, 2850.5, 2210.9, 1690.4, 1630.1, 1553.9, 1522.2, 1502.6, 1467.4, 1426.6, 1374.4, 1334.5, 1262.2, 1236.3, 1197.0, 1120.1, 1042.1, 994.2, 848.9, 822.8, 721.1, 626.8, 541.8; MS (70 eV, EI): calcd for $C_{53}H_{87}N_3O_5$, 846.27; found, 846 (M^+).

*1-Hexyl-6-[(trimethylsilyl)ethynyl]uracil (**7**)*: Dry NEt_3 (45 mL) and toluene (45 mL) were added to a Shlenk tube. The solution was degassed by one freeze-pump-thaw cycle. Idoduracil derivative **6** (1.22 g, 4.65 mmol),

$[(Ph_3P)_2PdCl_2]$ (0.16 g, 0.23 mmol), and CuI (0.1 g, 0.47 mmol) were then added and the solution degassed a second time. Finally, ethynyltrimethylsilane (2.5 mL, 18.63 mmol) was added, the reaction mixture degassed one last time and the whole mixture stirred overnight at rt under Ar. The resulting dark mixture was filtered over celite and washed with toluene (50 mL). Removal of the solvents under vacuum and purification of the crude by CC (cyclohexane/AcOEt 9:1/8:2/7:3) yielded compound **7** (0.66 g, 60%) as a brown solid. m.p. 100–104 °C; ^{1}H NMR (200 MHz, $CDCl_3$, δ):10.08 (br, 1H; CONHCO), 5.9 (s, 1H; COCH), 4 (t, 2H; $NCH_2(CH_2)_4CH_3$), 1.7 (m, 2H; $NCH_2CH_2(CH_2)_3CH_3$), 1.3 (m, 6H; $NCH_2CH_2(CH_2)_3CH_3$), 0.9 (t, 3H; $(CH_2)_5CH_3$), 0.3 (s, 9H; $Si(CH_3)_3$); ^{13}C NMR (50 MHz, $CDCl_3$, δ): 163.12; 150.92; 137.88; 108.06; 107.19; 94.67; 46.54; 31.46; 28.72; 26.34; 22.57; 14.03; 0.73; IR (cm^{-1}): $\nu = 3422.2$; 3149.1; 3096.6; 3018.6; 2959.4; 2929.2; 2860.0; 2798.0; 1715.2; 1682.6; 1584.2; 1462.9; 1416.6; 1362.6; 1248.8; 1185.8; 856.8; 825.4; 760.1; 563.1; MS (70 eV, EI): calcd for $C_{15}H_{24}N_2O_2Si$, 292.45; found, 292(M^+).

FT-IR Measurements: Infrared spectra were taken by a Bruker Tensor 78 and IFS66v FT-IR instrument in KBr pellets in the mid-infrared range (above 400 cm^{-1}) and neat samples between polyethylene disks in the far-infrared range (below 500 cm^{-1}) with 2 cm^{-1} resolution. The pellets typically contained 1–2-mg material in 400-mg KBr. The spectra shown are baseline-corrected and normalized to the molar concentration of the pellets. The temperature was regulated in a liquid nitrogen flow-through cryostat.

Scanning Tunnelling Microscopy: STM measurements at the liquid–solid interface were carried out both in constant height and in constant current modes using a DI multimode microscope (Veeco). The STM tips were mechanically cut from a Pt:Ir (80:20) wire. Samples were prepared by depositing a droplet of solution on freshly cleaved highly oriented pyrolytic graphite (HOPG). The first solution containing molecule **2** (0.5 mM) was prepared by mixing a few droplets of $CHCl_3$ with 5 mL of ultra pure *n*-tetradecane while the solution containing molecule **1** (0.6 mM), as well as the solution containing the [**1**·**2**] dimers (4 mM of molecule **1** and 0.4 mM of molecule **2**), were obtained from a few droplets of toluene mixed with 5 mL of 1-phenyloctane.The preparation of the pentamer monolayer was done first by forming one monolayer of **1** on HOPG followed by consecutive deposition of molecule **3** from a solution made of 300 μL of toluene, a few droplets of DMSO, and 3 mL of 1-phenyloctane. The raw STM data were processed by the application of background flattening and the drift was corrected using the underlying graphite lattice as a reference. The latter lattice was imaged underneath the molecules by lowering the bias voltage to 20 mV and raising the average tunnelling current to 65 pA. All molecule models were corrected by cycles of geometrical minimization with the MM2 force field with a conversion gradient of 0.5 rms kcal mol^{-1}.

Acknowledgements

This work was financially supported by the European Union through the Marie-Curie RTNs PRAIRIES (MRTN-CT-2006-035810) and EST–SUPER (MEST-CT-2004-008128), MIUR (Firb RBIN04HC3S), INSTM, the Belgian National Research Foundation (FRS-FNRS) and ''Loterie Nationale'' (through the contracts n° 2.4.625.08 and 2.4.550.09), the University of Namur, the ERA-Chemistry project SurConFold project. ALP thanks Università di Trieste for the doctoral fellowship. We are grateful to Prof. C. A. Hunter for providing us with his software for the evaluation of the binding data. Supporting Information is available online from Wiley InterScience or from the author.

Received: September 23, 2008
Revised: January 14, 2009
Published online: February 27, 2009

[1] Special issue on ''Supramolecular Chemistry and Self-Assembly'', *Science* **2002**, *295*, 2396.
[2] Special issue on ''Supramolecular Chemistry and Self-Assembly'', *Proc. Natl. Acad. Sci. USA* **2002**, *99*, 4762.
[3] Special issue on ''Supramolecular Approaches to Organic Electronics and Nanotechnology'', *Adv. Mater.* **2006**, *18*, 1227.
[4] Special issue ''Supramolecular Chemistry Anniversary'', *Chem. Soc. Rev.* **2007**, *36*, 125.
[5] F. Rosei, M. Schunack, Y. Naitoh, P. Jiang, A. Gourdon, E. Laegsgaard, I. Stensgaard, C. Joachim, F. Besenbacher, *Prog. Surf. Sci.* **2003**, *71*, 95.
[6] F. Rosei, *J. Phys. Condens. Matter* **2004**, *16*, S1373.
[7] J. V. Barth, G. Costantini, K. Kern, *Nature* **2005**, *437*, 671.
[8] D. Bonifazi, A. Kiebele, M. Stöhr, F. Cheng, T. Jung, F. Diederich, H. Spillmann, *Adv. Funct. Mater.* **2007**, *17*, 1051.
[9] M. Surin, P. Samorì, *Small* **2007**, *3*, 190.
[10] J. V. Barth, *Annu. Rev. Phys. Chem.* **2007**, *58*, 375.
[11] L. Piot, D. Bonifazi, P. Samorì, *Adv. Funct. Mater.* **2007**, *17*, 3689.
[12] S. Ito, M. Wehmeier, J. D. Brand, C. Kubel, R. Epsch, J. P. Rabe, K. Müllen, *Chem. Eur. J.* **2000**, *6*, 4327.
[13] T. Yokoyama, S. Yokoyama, T. Kamikado, Y. Okuno, S. Mashiko, *Nature* **2001**, *413*, 619.
[14] M. de Wild, S. Berner, H. Suzuki, H. Yanagi, D. Schlettwein, S. Ivan, A. Baratoff, H. J. Guentherodt, T. A. Jung, *ChemPhysChem* **2002**, *3*, 881.
[15] N. Wintjes, D. Bonifazi, F. Y. Cheng, A. Kiebele, M. Stöhr, T. Jung, H. Spillmann, F. Diederich, *Angew. Chem. Int. Ed.* **2007**, *46*, 4089.
[16] M. Linares, L. Scifo, R. Demadrille, P. Brocorens, D. Beljonne, R. Lazzaroni, B. Grevin, *J. Phys. Chem. C* **2008**, *112*, 6850.
[17] Y. H. Wei, W. J. Tong, M. B. Zimmt, *J. Am. Chem. Soc.* **2008**, *130*, 3399.
[18] N. Lin, A. Dmitriev, J. Weckesser, J. V. Barth, K. Kern, *Angew. Chem. Int. Ed.* **2002**, *41*, 4779.
[19] S. De Feyter, M. M. S. Abdel-Mottaleb, N. Schuurmans, B. J. V. Verkuijl, J. H. van Esch, B. L. Feringa, F. C. De Schryver, *Chem. Eur. J.* **2004**, *10*, 1124.
[20] P. Zell, F. Mogele, U. Ziener, B. Rieger, *Chem. Eur. J.* **2006**, *12*, 3847.
[21] B. A. Hermann, L. J. Scherer, C. E. Housecroft, E. C. Constable, *Adv. Funct. Mater.* **2006**, *16*, 221.
[22] G. R. Newkome, P. S. Wang, C. N. Moorefield, T. J. Cho, P. P. Mohapatra, S. N. Li, S. H. Hwang, O. Lukoyanova, L. Echegoyen, J. A. Palagallo, V. Iancu, S. W. Hla, *Science* **2006**, *312*, 1782.
[23] U. Schlickum, R. Decker, F. Klappenberger, G. Zoppellaro, S. Klyatskaya, M. Ruben, I. Silanes, A. Arnau, K. Kern, H. Brune, *Nano Lett.* **2007**, *7*, 3813.
[24] M. Surin, P. Samorì, A. Jouaiti, N. Kyritsakas, M. W. Hosseini, *Angew. Chem. Int. Ed.* **2007**, *46*, 245.
[25] G. Gottarelli, S. Masiero, E. Mezzina, S. Pieraccini, J. P. Rabe, P. Samorì, G. P. Spada, *Chem. Eur. J.* **2000**, *6*, 3242.
[26] J. V. Barth, J. Weckesser, C. Z. Cai, P. Gunter, L. Burgi, O. Jeandupeux, K. Kern, *Angew. Chem. Int. Ed.* **2000**, *39*, 1230.
[27] S. De Feyter, A. Gesquiere, M. M. Abdel-Mottaleb, P. C. M. Grim, F. C. De Schryver, C. Meiners, M. Sieffert, S. Valiyaveettil, K. Müllen, *Acc. Chem. Res.* **2000**, *33*, 520.
[28] T. Giorgi, S. Lena, P. Mariani, M. A. Cremonini, S. Masiero, S. Pieraccini, J. P. Rabe, P. Samorì, G. P. Spada, G. Gottarelli, *J. Am. Chem. Soc.* **2003**, *125*, 14741.
[29] S. Griessl, M. Lackinger, M. Edelwirth, M. Hietschold, W. M. Heckl, *Single Mol.* **2002**, *3*, 25.
[30] J. Lu, Q. D. Zeng, C. Wang, Q. Y. Zheng, L. J. Wan, C. L. Bai, *J. Mater. Chem.* **2002**, *12*, 2856.
[31] Z. Ma, Y. Y. Wang, P. Wang, W. Huang, Y. B. Li, S. B. Lei, *ACS Nano* **2007**, *1*, 160.
[32] C. Meier, U. Ziener, K. Landfester, P. Weihrich, *J. Phys. Chem. B* **2005**, *109*, 21015.
[33] G. Pawin, K. L. Wong, K. Y. Kwon, L. Bartels, *Science* **2006**, *313*, 961.
[34] M. Stöhr, M. Wahl, C. H. Galka, T. Riehm, T. A. Jung, L. H. Gade, *Angew. Chem. Int. Ed.* **2005**, *44*, 7394.
[35] F. Tao, S. L. Bernasek, *Langmuir* **2007**, *23*, 3513.
[36] L. P. Xu, J. R. Gong, L. J. Wan, T. G. Jiu, Y. L. Li, D. B. Zhu, K. Deng, *J. Phys. Chem. B* **2006**, *110*, 17043.

[37] S. Yoshimoto, N. Yokoo, T. Fukuda, N. Kobayashi, K. Itaya, *Chem. Commun.* **2006**, 500.
[38] H. Zhou, H. Dang, J. H. Yi, A. Nanci, A. Rochefort, J. D. Wuest, *J. Am. Chem. Soc.* **2007**, *129*, 13774.
[39] K. G. Nath, O. Ivasenko, J. M. MacLeod, A. Nanci, J. D. Wuest, D. F. Perepichka, F. Rosei, *J. Phys. Chem. C* **2007**, *111*, 16996.
[40] Y. Okawa, M. Aono, *Nature* **2001**, *409*, 683.
[41] A. Miura, S. De Feyter, M. M. S. Abdel-Mottaleb, A. Gesquiere, P. C. M. Grim, G. Moessner, M. Sieffert, M. Klapper, K. Müllen, F. C. De Schryver, *Langmuir* **2003**, *19*, 6474.
[42] L. Grill, M. Dyer, L. Lafferentz, M. Persson, M. V. Peters, S. Hecht, *Nat. Nanotechnol.* **2007**, *2*, 687.
[43] N. A. A. Zwaneveld, R. Pawlak, M. Abel, D. Catalin, D. Gigmes, D. Bertin, L. Porte, *J. Am. Chem. Soc.* **2008**, *130*, 6678.
[44] M. Matena, T. Riehm, M. Stöhr, T. A. Jung, L. H. Gade, *Angew. Chem. Int. Ed.* **2008**, *47*, 2414.
[45] S. De Feyter, F. C. De Schryver, *Chem. Soc. Rev.* **2003**, *32*, 393.
[46] F. Cicoira, C. Santato, F. Rosei, *Top. Curr. Chem.* **2008**, *285*, 203.
[47] J. A. Theobald, N. S. Oxtoby, M. A. Phillips, N. R. Champness, P. H. Beton, *Nature* **2003**, *424*, 1029.
[48] L. M. A. Perdigão, N. R. Champness, P. H. Beton, *Chem. Commun.* **2006**, 538.
[49] C. A. Palma, M. Bonini, A. Llanes-Pallas, T. Breiner, M. Prato, D. Bonifazi, P. Samorì, *Chem. Commun.* **2008**, 5289.
[50] M. E. Cañas-Ventura, W. Xiao, D. Wasserfallen, K. Müllen, H. Brune, J. V. Barth, R. Fasel, *Angew. Chem. Int. Ed.* **2007**, *46*, 1814.
[51] K. G. Nath, O. Ivasenko, J. A. Miwa, H. Dang, J. D. Wuest, A. Nanci, D. F. Perepichka, F. Rosei, *J. Am. Chem. Soc.* **2006**, *128*, 4212.
[52] W. Mamdouh, M. Dong, S. Xu, E. Rauls, F. Besenbacher, *J. Am. Chem. Soc.* **2006**, *128*, 13305.
[53] H. Zhang, F. J. M. Hoeben, M. J. Pouderoijen, A. Schenning, E. W. Meijer, F. C. Schryver, S. De Feyter, *Chem. Eur. J.* **2006**, *12*, 9046.
[54] B. Feibush, A. Figueroa, R. Charles, K. D. Onan, P. Feibush, B. L. Karger, *J. Am. Chem. Soc.* **1986**, *108*, 3310.
[55] M.-J. Brienne, J. Gabard, J.-M. Lehn, I. Stibor, *J. Chem. Soc. Chem. Commun.* **1989**, 1868.
[56] M. Kotera, J.-M. Lehn, J. P. Vigneron, *J. Chem. Soc. Chem. Commun.* **1994**, 197.
[57] R. F. Service, P. Szuromi, J. Uppenbrink, *Science* **2002**, *295*, 2395.
[58] A. Llanes-Pallas, M. Matena, T. Jung, M. Prato, M. Stöhr, D. Bonifazi, *Angew. Chem. Int. Ed.* **2008**, *47*, 7726.
[59] A. Llanes-Pallas, C. A. Palma, L. Piot, A. Belbakra, A. Listorti, M. Prato, P. Samorì, N. Armaroli, D. Bonifazi, *J. Am. Chem. Soc.* **2004**, *126*, 177.
[60] L. J. Prins, D. N. Reinhoudt, P. Timmerman, *Angew. Chem. Int. Ed.* **2001**, *40*, 2382.
[61] X. Shi, K. M. Barkigia, J. Fajer, C. M. Drain, *J. Org. Chem.* **2001**, *66*, 6513.
[62] F. H. Beijer, R. P. Sijbesma, J. Vekemans, E. W. Meijer, H. Kooijman, A. L. Spek, *J. Org. Chem.* **1996**, *61*, 6371.
[63] K. Sonogashira, Y. Tohda, N. Hagihara, *Tetrahedron Lett.* **1975**, *16*, 4467.
[64] J. Wu, M. D. Watson, L. Zhang, Z. Wang, K. Mullen, *J. Am. Chem. Soc.* **2004**, *126*, 177.
[65] G. C. McGonigal, R. H. Bernhardt, D. J. Thomson, *Appl. Phys. Lett.* **1990**, *57*, 28.
[66] J. P. Rabe, S. Buchholz, *Science* **1991**, *253*, 424.
[67] H. Dang, M. A. Garcia-Garibay, *J. Am. Chem. Soc.* **2001**, *123*, 355.
[68] A. P. Bisson, C. A. Hunter, J. C. Morales, K. Young, *Chem. Eur. J.* **1998**, *4*, 845.
[69] R. P. Sijbesma, E. W. Meijer, *Chem. Commun.* **2003**, *9*, 5.
[70] G. A. Jeffrey, *An Introduction to Hydrogen Bonding*, Oxford University Press, Oxford **1997**.
[71] D. Hadzi, S. Bratos, *Vibrational Spectroscopy of the Hydrogen Bond*, North-Holland, Amsterdam **1976**.
[72] R. Langner, G. Zundel, *J. Phys. Chem. A* **1998**, *102*, 6635.
[73] A. J. Barnes, M. A. Stuckey, W. J. Orville-Thomas, *J. Mol. Struct.* **1979**, *56*, 14.
[74] W. S. Yang, S. G. Chen, X. D. Chai, Y. W. Cao, R. Lu, W. P. Chai, Y. S. Jiang, T. J. Li, J. M. Lehn, *Synth. Met.* **1995**, *71*, 2107.
[75] H. I. Abdulla, M. F. El-Bermani, *Spectrochim. Acta Part A* **2001**, *57*, 2659.
[76] B. Morzyk-Ociepa, M. J. Nowak, D. Michalska, *Spectrochim. Acta Part A* **2004**, *60*, 2113.
[77] K. Nakamoto, M. Margoshes, R. E. Rundle. *J. Am. Chem. Soc.* **1955**, *77*, 6480.
[78] A. V. Iogansen, *Spectrochim. Acta Part A* **1999**, *55*, 1585.
[79] M. Rozenberg, G. Shoham, I. Reva, R. Fausto, *Spectrochim. Acta Part A* **2004**, *60*, 2323.
[80] R. Bauer, G. Zundel, *J. Phys. Chem. A* **2002**, *106*, 5828.
[81] R. Lazzaroni, A. Calderone, J.-L. Brédas, J. P. Rabe, *J. Chem. Phys.* **1997**, *107*, 99.
[82] K. Perronet, F. Charra, *Surf. Sci.* **2004**, *551*, 213.